

Distribution Agreement

In presenting this thesis as a partial fulfillment of the requirements for a degree from Emory University, I hereby grant to Emory University and its agents the non-exclusive license to archive, make accessible, and display my thesis in whole or in part in all forms of media, now or hereafter now, including display on the World Wide Web. I understand that I may select some access restrictions as part of the online submission of this thesis. I retain all ownership rights to the copyright of the thesis. I also retain the right to use in future works (such as articles or books) all or part of this thesis.

Simon Jiang

April 10, 2023

Elucidating the composition and protein interactome of the *Candida albicans* eIF3 complex

by

Simon Jiang

Sohail Khoshnevis
Adviser

Chemistry

Sohail Khoshnevis
Adviser

Homa Ghalei
Committee Member

Matthew Weinschenk
Committee Member

2023

Elucidating the composition and protein interactome of the *Candida albicans* eIF3 complex

By

Simon Jiang

Sohail Khoshnevis

Adviser

An abstract of
a thesis submitted to the Faculty of Emory College of Arts and Sciences
of Emory University in partial fulfillment
of the requirements of the degree of
Bachelor of Science with Honors

Chemistry

2023

Abstract

Elucidating the composition and protein interactome of the *Candida albicans* eIF3 complex
By Simon Jiang

Candida albicans is a fungal pathogen responsible for a large proportion of nosocomial infections, especially in immunocompromised patients. Existing as a dimorphic organism, *C. albicans* is capable of undergoing a morphological transition that is critical for its virulence from budding yeast cells to elongated filaments called hyphae. While the transcriptional regulation that is associated with hyphae formation is well-documented, comparatively little is known about the translational regulation underlying this process. Transcript levels do not always predict protein expression during morphological transition, which indicates that there is translational regulation occurring that is not known yet, representing a crucial gap in knowledge regarding hyphae induction. An important protein complex associated with the most regulated step of translation, initiation, is eukaryotic initiation factor 3 (eIF3), which has been observed to coordinate other translation factors and selectively bind to certain mRNA transcripts among other duties. While there are similarities between the eIF3 of *C. albicans* and that of other eukaryotes, the compositions vary. Haploinsufficiency of eIF3 has been documented in *C. albicans*, which indicates the importance of this complex for the yeast-hyphae transition. To help uncover the contribution of eIF3 to translational regulation during hyphae induction in *C. albicans*, this work investigated the subunit composition of eIF3 in *C. albicans* as well as its protein interactome in different morphological stages. Using epitope tagging of the eIF3b subunit and subsequent immunoprecipitation, eIF3 in *C. albicans* was determined to comprise 9 of the 13 subunits found in human eIF3. Co-immunoprecipitation and mass spectrometry analysis determined the changes in the eIF3 proteome over time and the strength of those interactions. Alterations in the composition of eIF3 during hyphae formation were discovered, suggesting the existence of sub-populations of eIF3 in *C. albicans*. These findings provide insight into the unknown mechanisms by which eIF3 influences translation regulation in *C. albicans*, an area of study that may prove invaluable in the fight against this lethal pathogen.

Elucidating the composition and protein interactome of the *Candida albicans* eIF3 complex

By

Simon Jiang

Sohail Khoshnevis

Adviser

A thesis submitted to the Faculty of Emory College of Arts and Sciences
of Emory University in partial fulfillment
of the requirements of the degree of
Bachelor of Science with Honors

Chemistry

2023

Acknowledgements

Thank you to all the current and past members of the Ghalei lab for answering all my questions. Dr. Ghalei and Dr. Khoshnevis, thank you for supporting me through this thesis project. Thank you to the *C. albicans* for cooperating with my experiments.

Table of Contents

<i>Introduction</i>	1
<i>Methods</i>	4
E. coli Miniprep	4
PCR Amplification and Gel Electrophoresis	5
PCR Purification and DNA Precipitation	5
Yeast Transformation	5
Western blot	6
Cell culture harvesting	7
Affinity Purification	8
<i>Results</i>	8
eIF3 was HA-tagged and isolated	8
Protein interactome of eIF3 changes throughout hyphae formation	11
eIF3 composition changes throughout hyphae formation	14
<i>Discussion</i>	15
<i>References</i>	18

Introduction

Candida albicans is an opportunistic fungal pathogen that naturally inhabits moist mucosal surfaces on the human body, such as the gut, vagina, and oral cavity. Under normal circumstances, *C. albicans* is relatively harmless and does not cause sickness. Fungal infection caused by *C. albicans*, candidiasis, often occurs when there is a drastic disruption either in a host's microbiome or in a host's immune response¹, both of which are common in the hospital setting². Patients on immunosuppressant drugs and those who are otherwise immunocompromised often cannot control the spread and colonization of *C. albicans* on mucosal surfaces³. *Candida* species represent the fourth most common source of nosocomial bloodstream infections (BSI) in the United States, of which *C. albicans* comprise 45% of cases⁴. These cases have high variability between each other because *C. albicans* can invade at almost every orifice and even from within the body. Unfortunately, as risk factors for invasive fungal infections have increased in frequency⁵, *C. albicans* BSIs have also increased⁶. This worrying trend, coupled with growing resistance of *C. albicans* to antifungal agents^{7,8} and a devastating mortality rate of between 36-63%⁹, highlights the urgency of imminently pursuing research on *C. albicans*.

C. albicans exists as a dimorphic organism. Normally presenting as budding yeast cells, *C. albicans* has the ability to undergo a morphological transition induced under certain host conditions to filamentous strands called hyphae. The ability to rapidly change from yeast to hyphae allows *C. albicans* to adhere to cells, invade tissues, evade macrophages, and form biofilm¹⁰⁻¹⁴. To date, extensive research has characterized the transcriptome¹⁵⁻¹⁷ and proteome¹⁸⁻²¹ of *C. albicans* under different environmental conditions and has even defined crucial transcriptional processes that are associated with hyphae formation²²⁻²⁷. Analyses of

differentially expressed genes during morphological transition showed a general correlation between transcript and protein levels²⁸⁻³¹. However, the transcript and protein levels of several virulence factors follow opposite trends, suggesting that the expression of those factors are controlled translationally. This is not entirely unprecedented, as it is documented that mRNA transcript quantities do not always predict protein levels in eukaryotes³². However, the exact mechanism of post-transcriptional regulation that underlies this phenomenon during morphological transition is not known and presents a target for studying protein synthesis and its regulation in *C. albicans*.

To ensure the smooth flow of genetic information, regulation in eukaryotes occurs during transcription and translation. While transcriptional regulation is crucial, it is generally a slower process than translational regulation, which is more rapid and is critical during periods of dynamic transition, such as during responses to stress and changes in external stimuli^{32,33}. Translation can be split into three overarching steps, initiation, elongation, and termination. During the initiation phase of translation, with the help of several translation initiation factors, the ribosome binds to the mRNA and establishes the correct reading frame. During translation elongation, the ribosome moves along the mRNA to build the polypeptide chain. Translation termination occurs as the ribosome encounters the stop codon, at which point the newly synthesized peptide is released. Of the three, initiation is the most regulated step and is considered the major rate-limiting step in protein synthesis³⁴.

Eukaryotic initiation factor 3 (eIF3) is the largest and most complex initiation factor in eukaryotes. Importantly, eIF3 acts as a molecular scaffold for over 10 other initiation factors, guiding and interacting with them as they, along with the small ribosomal subunit, form the 43S preinitiation complex, which recognizes mRNA and locates the start codon^{35,36}. Recently, eIF3

has been implicated in a cap-dependent pathway of translation initiation by possessing the ability to interact with the 5' untranslated regions (5' UTR) of mRNA transcripts, allowing eIF3 to upregulate and downregulate select mRNA transcripts depending on the mode of binding^{37,38}. Further research has also uncovered that eIF3 can recognize select mRNA transcripts, allowing eIF3 to initiate translation without the need for canonical cap recognition between eIF4E and the mRNA transcript³⁹. Notably, hyphae induction of *C. albicans* cells were found to be stunted by drug-induced eIF3 haploinsufficiency, suggesting a link between eIF3 and translation of proteins required for hyphae formation⁴⁰.

As a recent bioinformatics analysis of *C. albicans* eIF3 suggested the presence of only 9 subunits, it is not clear how the *C. albicans* eIF3 compensates structurally for subunits only present in human eIF3 (eIF3d, e, k, l)⁴¹. eIF3 in humans is the most complex, comprising of 13 subunits (eIF3a-m), 6 of which are common to all eukaryotes (eIF3a, b, c, g, i, j)³⁴. The high-resolution cryo-EM structure of human eIF3 bound to the 48S initiation complex⁴² shows that each of the 7 non-common eIF3 subunits interact with the other eIF3 subunits and are crucial for the function of the entire complex. Since *C. albicans* lacks some of these subunits, it is unclear how its eIF3 forms and functions. One possibility is that the subunits are organized in a different configuration in space around the ribosome to fill in the gaps where additional subunits would be in humans. Alternatively, there may be separate factors that occupy the same space as these human-specific subunits that interact with eIF3.

The subunit composition and protein interactome of the *C. albicans* eIF3 protein complex are the major targets of investigation in this work. While the composition and interactome of human eIF3 is well documented^{30,43}, little is known about these aspects of eIF3 in *C. albicans*, which represents a major gap in understanding the role of eIF3 in regulating the transition from

yeast to hyphae in *C. albicans*. Recent literature has implicated eIF3 in several key regulatory pathways in translation initiation and mRNA transcript discrimination, which may point to the importance of eIF3 in guiding the translation of select mRNA transcripts during morphological transition³⁷. To determine the veracity of this overarching hypothesis, this work first generated a mutant strain of *C. albicans* containing an HA-epitope tagged eIF3 protein complex, specifically in the C-terminus of the eIF3b subunit. The resulting HA-tagged strain of *C. albicans* was used for the isolation of eIF3 complex by immunoprecipitation. The composition and protein interactome of the isolated complex was elucidated through liquid chromatography with tandem mass spectrometry. Immunoprecipitation at high salt concentration allowed for isolation of core eIF3 subunits and other tightly bound factors while immunoprecipitation at low salt concentration allowed for elucidation of more loosely bound proteins that would have been washed away at higher salt concentrations. The protein interactome of HA-tagged eIF3 at different salt concentrations was also compared between the yeast form of *C. albicans* and different stages of hyphae formation to generate preliminary data on the differences in eIF3-associating proteins in different morphological states.

Methods

E. coli Miniprep

5 mL *E. coli* containing plasmid pHA-NAT1⁴⁴, a plasmid incorporated with a human influenza hemagglutinin (HA) tag and nourseothricin N-acetyl transferase (NAT) selection marker, were incubated at 37° C for 16 hours in Luria Broth (LB) media and harvested. Cells were lysed and DNA was obtained using the High Pure Plasmid Isolation Kit⁴⁵.

PCR Amplification and Gel Electrophoresis

For all PCR amplifications, plasmid pHA-*NAT1* was used as the template DNA. 300 μ L PCR reactions contained 600 ng DNA, 0.5 μ M forward primer (AGAGATTATTGAAGAAAAAGAAGAAATTGTTGAAGGTGGTCGGATCCCCGGGTATTAA), 0.5 μ M reverse primer (CTATGGATTAAAAACTTTCTTTTGTTCGGTAATTCGTGTAAAACGACGGCCAGTGAA TTC), and 1x Q5 High-Fidelity Master Mix⁴⁶ containing 2 mM Mg²⁺ and proprietary Q5 High-Fidelity DNA polymerase. PCR amplification was confirmed on 1% agarose gels with DNA Marker Ladder II used as a molecular weight ladder. A Syngene InGenius3 gel imager was used to detect and visualize the gel.

PCR Purification and DNA Precipitation

Amplified DNA was purified using the High Pure PCR Product Purification Kit⁴⁷, with the replacement of Elution Buffer with Milli-Q (MQ) water. Purified DNA was precipitated at -80° C overnight with the addition of 0.1x volume of 3M sodium acetate and 3x volume of chilled 100% ethanol. Precipitated reaction was centrifuged at 21,100 xg for 45 minutes at 4° C. Supernatant was removed and the DNA pellet was washed with 500 μ L of chilled 80% ethanol. The solution was centrifuged at 21,100 xg for 45 minutes at 4° C and supernatant was removed. The DNA pellet was dried with the Eppendorf tube lid open at 42° C for 10 minutes. The DNA pellet was resuspended in 20 μ L (MQ) water.

Yeast Transformation

All steps in this procedure were performed sterilely near an open flame. Overnight 5 mL preculture of wild-type *C. albicans* in yeast extract-peptone-dextrose medium (YPD) was diluted to optical density, measured at 600 nm (OD₆₀₀), of 0.2 in 10 mL YPD and grown until mid-log phase (OD₆₀₀ 0.7). Cells were collected in a sterile 50 mL falcon tube and centrifuged at ~4,000

xg for 3 minutes at room temperature. Supernatant was decanted and the cell pellet was washed with 10 mL of MQ water. Cells were again centrifuged at ~4,000 xg for 3 minutes at room temperature. Supernatant was decanted and the cell pellet was washed with 5 mL of filter sterilized TE-LiAc solution (10 mM Tris pH 8.0, 1 mM EDTA, 100 mM LiAc). Cells were again centrifuged at ~4,000 xg for 3 minutes at room temperature. Supernatant was decanted and the cell pellet was resuspended via vortexing in the following solution: 5 μ L 10 mg/mL salmon sperm DNA, 20 μ L purified DNA, 70 μ L filter sterilized TE (100 mM Tris pH 8.0, 10 mM EDTA), 560 μ L fresh and filter sterilized 50% PEG 3350, 70 μ L filter sterilized 1M LiAc. The cell solution was then incubated at 30° C for 2 hours, heat shocked at 42° C for 15 minutes, and placed on ice for 2 minutes. The cell solution was added to 5 mL YPD and grown overnight at 30° C. The cell culture was transferred to a sterile 15 mL falcon tube and centrifuged at ~4,000 xg for 5 minutes at room temperature. Supernatant was removed and the cell pellet was resuspended in 300 μ L MQ water and evenly distributed onto 3 YPD-agar plates containing 100 μ g/mL NAT. Surviving colonies were restreaked using sterile wooden sticks onto new plates.

Western blot

Restreaked cell samples and a negative control wild-type strain were grown overnight in 5 mL YPD. 1 mL of cultured cells were centrifuged at 17,000 xg for 1 minute and supernatant was removed. Cell pellets were each resuspended in a mixture of 500 μ L SUMEB (1% SDS, 8 M Urea, 10 mM MOPS pH 6.8, 10 mM EDTA), 75 μ L β -mercaptoethanol, 5 μ L 1 mg/mL pepstatin A, 0.5 μ L 18 mg/mL PMSF, 0.5 μ L 20 mg/mL 1000x E64, 100 μ L silica disruption beads. Mixtures underwent three consecutive cycles of 1 minute vortex at 4° C, 1 minute rest in ice bath. The topmost 100 μ L of each solution was transferred to a new 1.5 mL Eppendorf tube and subsequently boiled at 95° C for 3 minutes. 20 μ L of each sample, alongside 3 μ L Precision dual

color ladder (BioRad) for reference, was analyzed on a 12% SDS-PAGE gel and transferred onto a nitrocellulose membrane via a semi-dry electrophoretic transfer. The membrane was then blocked in 3% milk in TBST solution (20 mM Tris, 150 mM NaCl, 0.1% Tween 20 detergent) to prevent nonspecific antibody binding and incubated overnight at 4° C in a 1:1000 dilution of primary antibody (α -HA raised in rat) in 3% milk in TBST solution. The membrane was then washed three times in 1x TBST solution while shaking for 10 minutes. The membrane was then incubated for 1 hour at room temperature in a 1:5000 dilution of secondary antibody (horseradish peroxidase-conjugated α -rat) in the same 3% milk solution as above. The membrane was washed three times in 1x TBST solution while shaking for 10 minutes and the chemiluminescence was detected using A Bio-Rad Chemidoc gel imager.

Cell culture harvesting

Restreaked cell samples and a wild-type strain were grown in 5 mL YPD and diluted to OD₆₀₀ 0.8 in RPMI 1640 media. Both control and experimental groups were grown in hyphae-inducing conditions (+10% fetal bovine serum at 37° C) and hyphae-restricting conditions (+10% MQ water at 30° C). Depending on the assay, cells were either harvested at various time points (0 hours, 1 hour, etc.) or at one predetermined time point. From this point on, all procedures were performed on ice. Ice cold water was added to fill the centrifuge bucket and slow down chemical reactions in the cells during the harvest. Immediately after centrifugation, supernatant was decanted, and cell pellets were transferred to 50 mL falcon tubes with ice-cold MQ water and centrifuged further. Cell pellets were weighed and lysis buffer (150 mM NaCl, 300 mM Tris pH 7.5, 0.075% NP40, 5 mM MgCl₂, 10 μ g/mL pepstatin A, 18 μ g/mL PMSF, 20 μ g/mL 1000x E64, cOmplete EDTA-free protease inhibitor cocktail [1 tablet per 10 mL lysis buffer]) was

added in a 1:1 volume to weight ratio. Samples were pipette-dripped into liquid nitrogen and frozen overnight at -80° C.

Affinity Purification

All steps in this procedure were performed cold. Frozen spheroid samples from the above procedure were systematically ground using mortar and pestle cooled by liquid nitrogen. The resultant fine powder was transferred to 1.5 mL Eppendorf tubes along with 1:1 v:w lysis buffer and 100 μ L silica disruption beads (RPI). Samples were thawed on a cold shaker and intermittently vortexed. Samples were then centrifuged at 6,000 xg for 5 minutes and supernatant was transferred to new 1.5 mL Eppendorf tubes. Samples were then centrifuged at 12,000 xg for 10 minutes and supernatant was transferred to new 1.5 mL Eppendorf tubes containing 50 μ L anti-HA magnetic beads equilibrated in lysis buffer. Samples were incubated on a cold shaker for 2 hours. From here, samples were washed 3x with 500 μ L different salt buffers (150-300 mM NaCl, 30 mM Tris pH 7.5, 0.075% NP40, 5 mM MgCl₂) depending on the assay. Samples were then washed 3x with 500 μ L 1x phosphate-buffered saline (PBS). 100 μ L of PBS was added to each sample, 50 μ L of which were sent for mass spectrometry analysis. The rest of the PBS was removed and eluted with 100 μ L of HA-peptide (1 mg/mL). These samples were incubated at 37° C for 10 minutes before visualization via Coomassie Blue staining.

Results

eIF3 was HA-tagged and isolated

To determine the composition and interactome of the eIF3 protein complex in *C. albicans*, epitope-tagged strains of the wild-type strain, SC5314, was first generated. An epitope was used as there is currently no readily available antibody that has strong affinity for the eIF3

protein complex or any of its subunits. The human influenza hemagglutinin (HA) tag was chosen as the epitope due to its known characterization and extensive usage as an antibody epitope tag⁴⁸. Additionally, a nourseothricin N-acetyl transferase (NAT) selection marker gene was inserted alongside the HA tag as the nourseothricin antibiotic is lethal to *C. albicans*⁴⁹. Theoretically, colonies that survive on a NAT plate should express the NAT gene and, therefore, have an HA-tagged eIF3. Plasmid pHA-NAT1, a vector containing the HA-tag and NAT marker gene, was used as a DNA template to insert the tag into the eIF3b subunit. Oligonucleotides 537 and 538, the forward and reverse primers, respectively, bound to regions in HA and NAT genes on the plasmid. These primers also contained 70 nucleotides of overhang at the 5' and 3' ends homologous to sequences immediately upstream and downstream of the eIF3b stop codon. This location was chosen due to past success in tagging and isolating eIF3 in *Saccharomyces cerevisiae*^{50,51}. Visualization of the DNA fragment on 1% agarose gel compared to a molecular weight ladder indicated that the PCR was successful and that the product was the correct size of around 3.7 kbp³⁸ (**Figure 1**). Successful incorporation of the eIF3b-HA tag was validated through Western blot. Proteins run on SDS gels were blocked with 3% milk in TBST to help reduce nonspecific binding of the antibody and incubated with α -HA antibody, which is itself a target for a chemiluminescent secondary antibody. Western blot of SC5314 cells transformed with an eIF3b-HA tag both presents bands that correspond with the predicted molecular weight of the eIF3b-HA subunit (**Figure 1**).

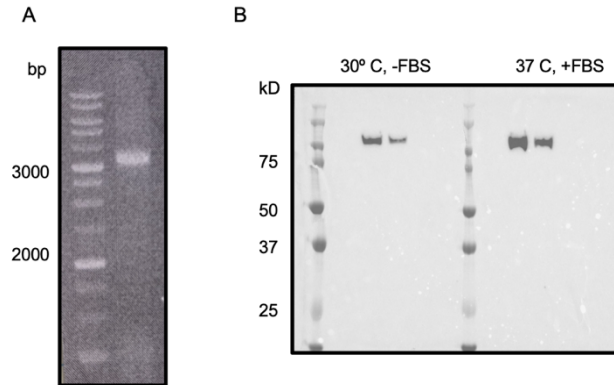


Figure 1. Gel confirmation of successful insertion of HA-NAT tag into *C. albicans* eIF3b subunit. **(A)** Amplified DNA fragment containing HA-NAT was visualized on 1% agarose gel to be the correct size of 3.7 kbp. **(B)** Western blot of SC5314 cells transformed with eIF3b-HA in hyphae-restricting (left) and hyphae-inducing (right) conditions using α -HA antibodies.

The successful generation of *C. albicans* strains expressing an eIF3b-HA tag allowed us to isolate and characterize the eIF3 complex in *C. albicans*. The composition and protein interactome of eIF3 were analyzed by purifying the eIF3 complex in high salt and low salt buffers, respectively. To confirm its composition, eIF3 was isolated and purified via immunoprecipitation. To select only for HA-tagged eIF3 in lysed cells, anti-HA conjugated magnetic beads were used. The beads were washed with 300 mM NaCl buffer and the protein was eluted with HA-peptide before being loaded onto an SDS gel. The predicted molecular weights of the various subunits of eIF3 in *C. albicans* is reflected in the separation of bands in the gel (**Figure 2**).

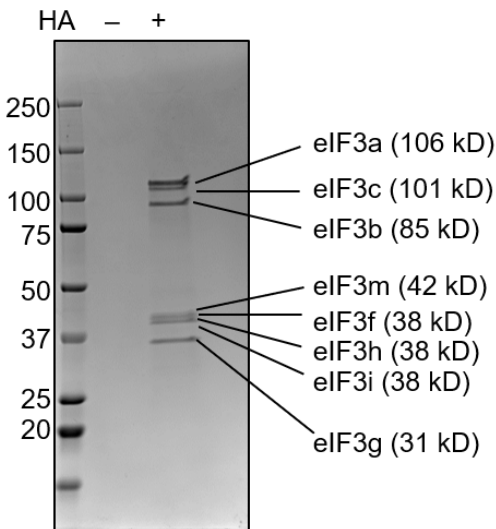


Figure 2. Affinity purification and immunoprecipitation of tagged eIF3 using magnetic beads. Mutant cells containing eIF3b-HA were harvested, lysed, and incubated with magnetic beads conjugated with α -HA antibody. Eluted sample was loaded and visualized on an SDS gel. Each band indicates the presence of a specific eIF3 subunit based on the predicted molecular weight.

Protein interactome of eIF3 changes throughout hyphae formation

To experimentally determine the composition of eIF3 in *C. albicans* and determine its protein interactome, cells in either yeast or at different time points in hyphae formation were grown in their respective conditions and harvested. Cells were grown in a mixture of RPMI 1640 media and fetal bovine serum (FBS) at 37° C to induce hyphae formation. The yeast control group grew in the absence of FBS at 30° C. eIF3 was co-immunoprecipitated at low, 150 mM, and high, 300 mM salt concentrations for each time interval. Washing with salt at a low concentration would retain proteins weakly interacting with eIF3 as the electrostatic interactions between these proteins and eIF3 would not be effectively disrupted, allowing for a glance into the protein interactome of eIF3. Using a highly concentrated salt buffer would introduce more disruptive salt ions that can break these weak ionic bonds but would keep the core eIF3 protein complex intact, allowing for isolation of just the eIF3 complex. Eluent samples from both assays

were sent directly for mass spectrometry analysis. After washes of 150 mM salt, 86 interacting proteins were found at a significant level (≥ 5 PSMs) in hyphae samples in addition to the core eIF3 subunits (Supplemental Data). 28 proteins other than the core eIF3 subunits were found at a significant level in hyphae samples after 300 mM salt washes (Supplemental Data).

Harvesting each culture at different time intervals allowed for comparison of relative protein levels in yeast and hyphae over time. Relative protein abundance was determined by normalizing PSM values at 1 and 2 hour marks with those harvested at 0 hours and comparing the difference in ratios. Variations in relative protein abundance between different proteins were determined by normalizing the PSM ratios of all proteins to the average of the PSM ratios of the core eIF3 subunits at every time point. This method allows for the quantification of changes in protein levels at different intervals relative to eIF3 levels even if there are variations in global protein quantities between samples. Proteins with significant changes in abundance ($\geq 15\%$ change) relative to eIF3 were identified after washes of 150 mM and 300 mM salt buffers (Figure 3). Many of these were identified to be kinases, RNA binding proteins, and other initiation factors.

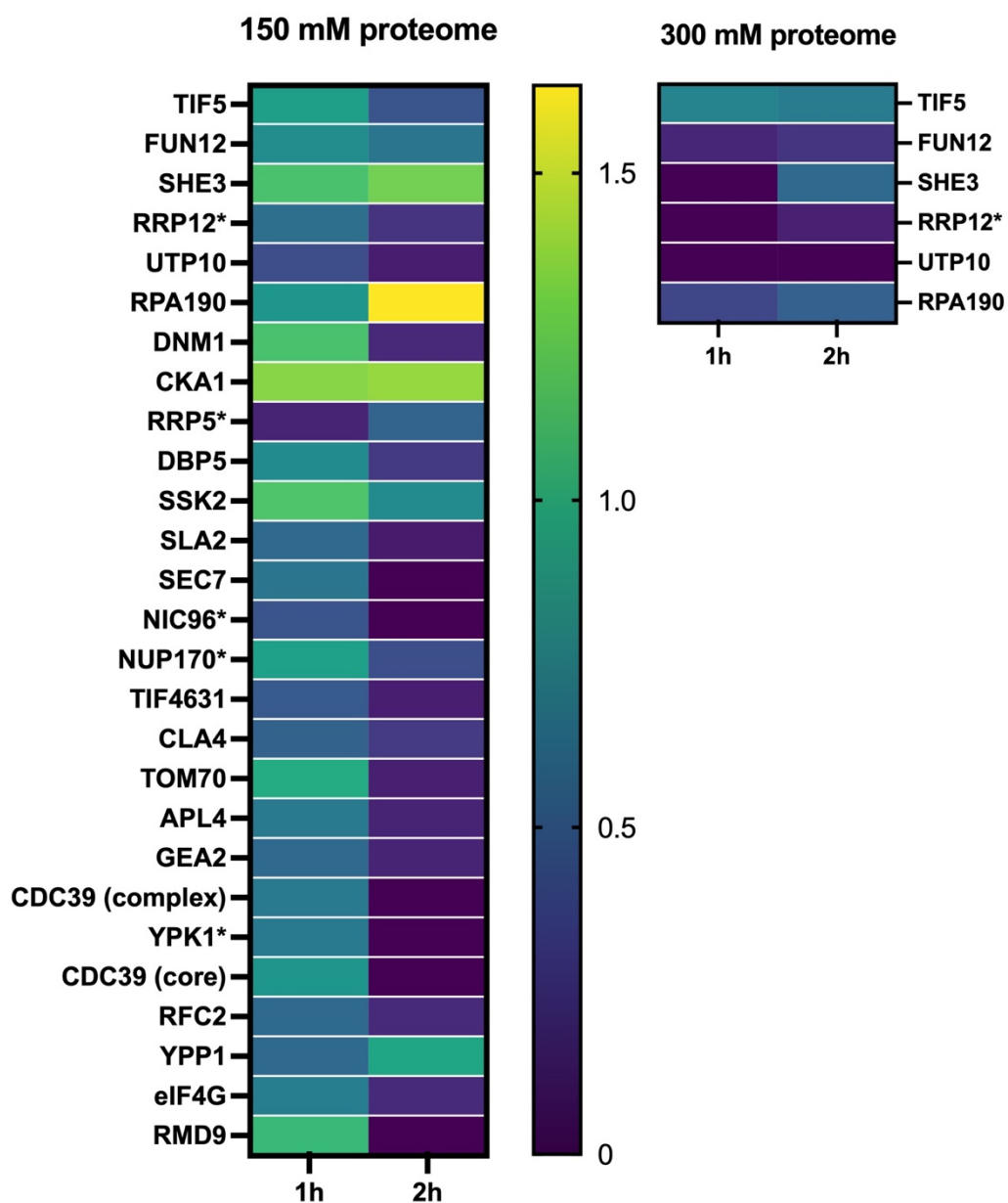


Figure 3. Heat map of relative abundances of significant eIF3 interacting proteins over time. eIF3b from hyphae cells were immunoprecipitated and washed at two salt concentrations, 150 mM and 300 mM. Relative protein abundances over time were normalized to average core eIF3 subunit abundance such that values > 1 indicate enhanced binding of proteins to eIF3 over time and that values < 1 indicate reduced eIF3 binding. Proteins in red for 300 mM salt washes signify that no appreciable quantity was recognized by mass spectrometry. * ortholog in *S. cerevisiae*.

eIF3 composition changes throughout hyphae formation

Variability in core eIF3 subunit relative abundance was also measured (Figure 4). Notably, eIF3j was found to drastically decrease in relative abundance over time compared to the rest of the subunits, an observation consistent with the finding that eIF3j is a substoichiometric, weakly associating subunit of the eIF3 complex^{52,53}. Additionally, eIF3 has a well-regulated ability to intentionally dissociate certain subunits³². This data shows that several of the subunits change in relative abundance over time after hyphae induction, suggesting that stoichiometric ratios of some subunits may change over time as *C. albicans* transitions to hyphae.

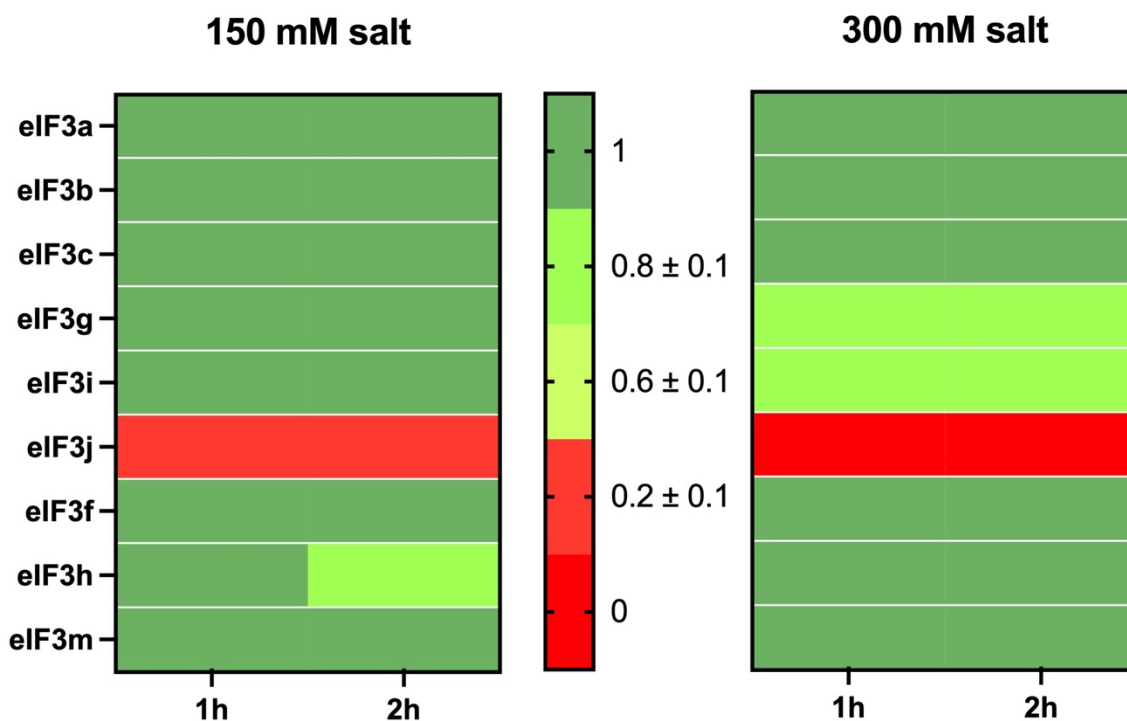


Figure 4. Heat map of relative abundances of core eIF3 subunits over time. eIF3b from hyphae cells were immunoprecipitated and washed at two salt concentrations, 150 mM and 300 mM. Relative protein abundances over time were normalized to average core eIF3 subunit abundance such that values < 1 indicate reduced protein binding to eIF3. Several relative abundances of select eIF3 subunits show visible change when washed with 150 mM and 300 mM salt.

Discussion

As one of the most common causes of nosocomial bloodstream infections for the past several decades, *Candida albicans* simultaneously represents a growing threat in medicine in that both risk factors for candidiasis as well as resistance to antifungal drug agents have increased recently. A recent study revealed that the expression of many virulent factors is controlled at the translation level³¹. However, little is known about the translational regulation that allows *C. albicans* to transition to hyphae and develop virulence. This work has taken the first step in elucidating the role of eIF3 in *C. albicans*, which is suspected to modulate the translational efficiency of select mRNA transcripts based on prior literature and preliminary data. Successful tagging of the eIF3b subunit with an HA epitope in SC5314 strain has led to the generation of a new mutant strain available for a multitude of different assays in the future. Pulling down HA-tagged eIF3 through immunoprecipitation allowed for characterization of the core subunits of eIF3 in *C. albicans*, which have before only been predicted through bioinformatics analysis.

Mass spectrometry analysis of the protein interactome of eIF3 has highlighted several interesting proteins. While the abundances of the majority of identified proteins decreased over time relative to eIF3, 2 proteins, She3 and Cka1, were found to increase in abundance after both 1 and 2 hours. She3 is crucial for select mRNA localization in *S. cerevisiae* by allowing for the joining of mRNA bound to She2 with Myo4, a myosin motor^{54,55}. She3 was found associated to eIF3 in significant quantities after washing at high salt concentrations, indicating that it is strongly associating with eIF3 and may play a role in directing mRNAs bound to eIF3 for selective spatial translation. Cka1 is the catalytic subunit of Casein kinase 2 (CK2), a ubiquitous kinase that is involved in cell growth and gene expression among many other functions⁵⁶. While CK2 has been documented to phosphorylate multiple translation initiation factors, such as eIF5⁵⁶

and eIF2 β ⁵⁷, it also phosphorylates several key residues in eIF3. The role of eIF3j in stabilizing and forming the eIF3 complex is promoted by CK2-phosphorylation⁵⁸. Additionally, CK2 phosphorylation of eIF3c allows for improved binding to other initiation factors, specifically eIF1, eIF2, and eIF5⁵⁹. While She3 and Cka1 were the only proteins identified that increased in relative abundance over time, eIF5 and eIF5B were found in high absolute quantities and were still bound to eIF3 after washing at high salt concentrations. Another major initiation factor, eIF5 promotes the hydrolysis of GTP that induces the dissociation of other initiation factors from the small ribosomal subunit^{35,60}. eIF5B, on the other hand, plays a role in joining the 43S pre-initiation complex with the 60S ribosomal subunit⁶¹. Due to their respective roles in facilitating the transition from translation initiation to elongation, eIF5 and eIF5b represent potential targets for eIF3 to regulate translation initiation further. It is possible that eIF3 prevents the dissociation of initiation factors from the ribosome. This supports a previous finding that eIF3 can stay bound to the ribosome to facilitate downstream reinitiation⁶². Regardless, further investigations must be conducted to discover the role of these proteins in interacting with eIF3.

The preliminary results illustrated in this thesis represent new promising avenues of research into the heterogeneity of the composition and proteome of eIF3 in *C. albicans* throughout hyphae formation. Immediate next steps in exploring the eIF3 protein complex is to design a double-tagged eIF3 complex, which would allow for the isolation of eIF3 complexes lacking different subunits and analysis of their protein and RNA interactome. eIF3 has shown to exhibit RNA-binding properties for the purposes of translation initiation³⁷. To investigate the RNA interactome in *C. albicans*, photoactivatable-ribonucleoside enhanced cross linking and immunoprecipitation (PAR-CLIP) can be utilized to pull down RNA transcripts that interact with eIF3⁶³. In PAR-CLIP a photoactivatable ribonucleoside, most commonly 4-thiouridine (4SU), is

inserted into RNA transcripts. When cells are subjected to ultraviolet radiation, 4SU effectively crosslinks to interacting proteins. While RNA transcripts have the ability to crosslink with interacting proteins naturally under UV light, 4SU enhances the efficiency of crosslinking such that subsequent RNA pull down via immunoprecipitation would generate a larger quantity of RNA.

To better understand the mechanism of action of eIF3 during translation initiation, the three-dimensional structure of *C. albicans* eIF3 bound to the ribosome has also yet to be solved, which represents another future endeavor. With the confirmation of the composition of eIF3, single-particle electron cryo-microscopy can be utilized to determine the structure of the whole eIF3 complex as well as its sub-populations with high resolution⁶⁴. eIF3 is emerging as a promising drug target^{33,65,66}. Further analysis of eIF3 interactions and structure offer insight into new therapeutic avenues. The generation of an eIF3 tagged strain of *C. albicans* in this work, along with preliminary data regarding the composition and protein interactome of eIF3, has built a foundation for future research endeavors into the complex translational machinery that drives the pathogenicity of *C. albicans*.

References

- (1) Tsui, C.; Kong, E. F.; Jabra-Rizk, M. A. Pathogenesis of *Candida albicans* biofilm. *Pathogens and Disease* **2016**, *74* (4), 1-13.
- (2) Williams, D. W.; Jordan, R. P. C.; Wei, X.-Q.; Alves, C. T.; Wise, M. P.; Wilson, M. J.; Lewis, M. A. O. Interactions of *Candida Albicans* with Host Epithelial Surfaces. *Journal of Oral Microbiology* **2013**, *5* (1), 22434.
- (3) Gow, N. A. R.; van de Veerdonk, F. L.; Brown, A. J. P.; Netea, M. G. *Candida Albicans* Morphogenesis and Host Defence: Discriminating Invasion from Colonization. *Nature Reviews Microbiology* **2011**, *10* (2), 112–122.
- (4) Hajjeh, R. A.; Sofair, A. N.; Harrison, L. H.; Lyon, G. M.; Arthington-Skaggs, B. A.; Mirza, S. A.; Phelan, M.; Morgan, J.; Lee-Yang, W.; Ciblak, M. A.; Benjamin, L. E.; Thomson Sanza, L.; Huie, S.; Yeo, S. F.; Brandt, M. E.; Warnock, D. W. Incidence of Bloodstream Infections due to *Candida* Species and in Vitro Susceptibilities of Isolates Collected from 1998 to 2000 in a Population-Based Active Surveillance Program. *Journal of Clinical Microbiology* **2004**, *42* (4), 1519–1527.
- (5) Perlroth, J.; Choi, B.; Spellberg, B. Nosocomial Fungal Infections: Epidemiology, Diagnosis, and Treatment. *Medical Mycology* **2007**, *45* (4), 321–346.
- (6) Zheng, Y.-J.; Xie, T.; Wu, L.; Liu, X.-Y.; Zhu, L.; Chen, Y.; Mao, E.-Q.; Han, L.-Z.; Chen, E.-Z.; Yang, Z.-T. Epidemiology, Species Distribution, and Outcome of Nosocomial *Candida* Spp. Bloodstream Infection in Shanghai: An 11-Year Retrospective Analysis in a Tertiary Care Hospital. *Annals of Clinical Microbiology and Antimicrobials* **2021**, *20* (1).
- (7) Taff, H. T.; Mitchell, K. F.; Edward, J. A.; Andes, D. R. Mechanisms of *Candida* Biofilm Drug Resistance. *Future Microbiology* **2013**, *8* (10), 1325–1337.
- (8) Shapiro, R. S.; Robbins, N.; Cowen, L. E. Regulatory Circuitry Governing Fungal Development, Drug Resistance, and Disease. *Microbiology and Molecular Biology Reviews* **2011**, *75* (2), 213–267.
- (9) Flevari, A.; George, D.; Theodorakopoulou, M.; Velegaki, A.; Armaganidis, A. Treatment of Invasive Candidiasis in the Elderly: A Review. *Clinical Interventions in Aging* **2013**, *8*, 1199.
- (10) Mitchell, A. P. Dimorphism and Virulence in *Candida Albicans*. *Current Opinion in Microbiology* **1998**, *1* (6), 687–692.
- (11) Thompson, D. S.; Carlisle, P. L.; Kadosh, D. Coevolution of Morphology and Virulence in *Candida* Species. *Eukaryotic Cell* **2011**, *10* (9), 1173–1182.
- (12) Kumamoto, C. A.; Vences, M. D. Contributions of Hyphae and Hypha-Co-Regulated Genes to *Candida Albicans* Virulence. *Cellular Microbiology* **2005**, *7* (11), 1546–1554.
- (13) Ramage, G.; Saville, S. P.; Thomas, D. P.; López-Ribot, J. L. *Candida* Biofilms: An Update. *Eukaryotic Cell* **2005**, *4* (4), 633–638.
- (14) Kadosh, D. Regulatory Mechanisms Controlling Morphology and Pathogenesis in *Candida Albicans*. *Current Opinion in Microbiology* **2019**, *52*, 27–34.
- (15) Bruno, V. M.; Wang, Z.; Marjani, S. L.; Euskirchen, G. M.; Martin, J.; Sherlock, G.; Snyder, M. Comprehensive Annotation of the Transcriptome of the Human Fungal Pathogen *Candida Albicans* Using RNA-Seq. *Genome Research* **2010**, *20* (10), 1451–1458.
- (16) Short, B.; Delaney, C.; McKlound, E.; Brown, J. L.; Kean, R.; Litherland, G. J.; Williams, C.; Martin, S. L.; MacKay, W. G.; Ramage, G. Investigating the Transcriptome of *Candida Albicans* in a Dual-Species *Staphylococcus Aureus* Biofilm Model. *Frontiers in Cellular and Infection Microbiology* **2021**, *11*.

- (17) Wang, J.; Woodruff, R.; Dunn, M.; Fillinger, R.; Bennett, R.; Anderson, M. Intraspecies Transcriptional Profiling Reveals Key Regulators of *Candida Albicans* Pathogenic Traits. *mBio* **2021**, *12* (2).
- (18) Premisler, T.; Zahedi, R. P.; Lewandrowski, U.; Sickmann, A. Recent Advances in Yeast Organelle and Membrane Proteomics. *PROTEOMICS* **2009**, *9* (20), 4731–4743.
- (19) Truong, T.; Pang, L. M.; Rajan, S.; Wong, S. S. W.; Fung, Y. M. E.; Samaranyake, L.; Seneviratne, C. J. The Proteome of Community Living *Candida Albicans* Is Differentially Modulated by the Morphologic and Structural Features of the Bacterial Cohabitants. *Microorganisms* **2020**, *8* (10), 1541.
- (20) Abdulghani, M.; Iram, R.; Chidrawar, P.; Bhosle, K.; Kazi, R.; Patil, R.; Kharat, K.; Zore, G. Proteomic Profile of *Candida Albicans* Biofilm. *Journal of Proteomics* **2022**, *265*, 104661.
- (21) Amador-García, A.; Zapico, I.; Borrajo, A.; Malmström, J.; Monteoliva, L.; Gil, C. Extending the Proteomic Characterization of *Candida Albicans* Exposed to Stress and Apoptotic Inducers through Data-Independent Acquisition Mass Spectrometry. *mSystems* **2021**, *6* (5).
- (22) Kadosh, D.; Johnson, A. D. Induction of the *Candida Albicans* Filamentous Growth Program by Relief of Transcriptional Repression: A Genome-Wide Analysis. *Molecular Biology of the Cell* **2005**, *16* (6), 2903–2912.
- (23) Liu, Z.; Moran, G. P.; Sullivan, D. J.; MacCallum, D. M.; Myers, L. C. Amplification of TLO Mediator Subunit Genes Facilitate Filamentous Growth in *Candida* Spp. *PLOS Genetics* **2016**, *12* (10), e1006373.
- (24) Jenull, S.; Tscherner, M.; Gulati, M.; Nobile, C. J.; Chauhan, N.; Kuchler, K. The *Candida Albicans* HIR Histone Chaperone Regulates the Yeast-To-Hyphae Transition by Controlling the Sensitivity to Morphogenesis Signals. *Scientific Reports* **2017**, *7* (1).
- (25) Veri, A. O.; Miao, Z.; Shapiro, R. S.; Tebbji, F.; O’Meara, T. R.; Kim, S. H.; Colazo, J.; Tan, K.; Vyas, V. K.; Whiteway, M.; Robbins, N.; Wong, K. H.; Cowen, L. E. Tuning Hsf1 Levels Drives Distinct Fungal Morphogenetic Programs with Depletion Impairing Hsp90 Function and Overexpression Expanding the Target Space. *PLOS Genetics* **2018**, *14* (3), e1007270.
- (26) Ernst, J. F. Transcription Factors in *Candida Albicans* – Environmental Control of Morphogenesis. *Microbiology* **2000**, *146* (8), 1763–1774.
- (27) Villa, S.; Hamideh, M.; Weinstock, A.; Qasim, M. N.; Hazbun, T. R.; Sellam, A.; Hernday, A. D.; Thangamani, S. Transcriptional Control of Hyphal Morphogenesis in *Candida Albicans*. *FEMS Yeast Research* **2020**, *20* (1).
- (28) Grumaz, C.; Lorenz, S.; Stevens, P.; Lindemann, E.; Schöck, U.; Retey, J.; Rupp, S.; Sohn, K. Species and Condition Specific Adaptation of the Transcriptional Landscapes in *Candida Albicans* and *Candida Dubliensis*. *BMC Genomics* **2013**, *14* (1), 212.
- (29) Heilmann, C. J.; Sorgo, A. G.; Siliakus, A. R.; Dekker, H. L.; Brul, S.; de Koster, C. G.; de Koning, L. J.; Klis, F. M. Hyphal Induction in the Human Fungal Pathogen *Candida Albicans* Reveals a Characteristic Wall Protein Profile. *Microbiology* **2011**, *157* (8), 2297–2307.
- (30) Aoki, W.; Ueda, T.; Tatsukami, Y.; Kitahara, N.; Morisaka, H.; Kuroda, K.; Ueda, M. Time-Course Proteomic Profile Of *Candida Albicans* during Adaptation to a Fetal Serum. *Pathogens and Disease* **2012**, *67* (1), 67–75.

- (31) Mundodi, V.; Choudhary, S.; Smith, A. D.; Kadosh, D. Global Translational Landscape of the *Candida Albicans* Morphological Transition. *G3 Genes|Genomes|Genetics* **2020**, *11* (2).
- (32) Genuth, N. R.; Barna, M. The Discovery of Ribosome Heterogeneity and Its Implications for Gene Regulation and Organismal Life. *Molecular Cell* **2018**, *71* (3), 364–374.
- (33) Hao, P.; Yu, J.; Ward, R.; Liu, Y.; Hao, Q.; An, S.; Xu, T. Eukaryotic Translation Initiation Factors as Promising Targets in Cancer Therapy. *Cell Communication and Signaling* **2020**, *18* (1).
- (34) Rodnina, M. V. The Ribosome in Action: Tuning of Translational Efficiency and Protein Folding. *Protein Science* **2016**, *25* (8), 1390–1406.
- (35) Pestova, T. V.; Kolupaeva, V. G.; Lomakin, I. B.; Pilipenko, E. V.; Shatsky, I. N.; Agol, V. I.; Hellen, C. U. T. Molecular Mechanisms of Translation Initiation in Eukaryotes. *Proceedings of the National Academy of Sciences* **2001**, *98* (13), 7029–7036.
- (36) Hinnebusch, A. G. EIF3: A Versatile Scaffold for Translation Initiation Complexes. *Trends in Biochemical Sciences* **2006**, *31* (10), 553–562.
- (37) Lee, A. S. Y.; Kranzusch, P. J.; Cate, J. H. D. EIF3 Targets Cell-Proliferation Messenger RNAs for Translational Activation or Repression. *Nature* **2015**, *522* (7554), 111–114.
- (38) Cate, J. H. D. Human EIF3: From “Blobology” to Biological Insight. *Philosophical Transactions of the Royal Society B: Biological Sciences* **2017**, *372* (1716), 20160176.
- (39) Lee, A. S. Y.; Kranzusch, P. J.; Doudna, J. A.; Cate, J. H. D. EIF3d Is an mRNA Cap-Binding Protein That Is Required for Specialized Translation Initiation. *Nature* **2016**, *536* (7614), 96–99.
- (40) Oh, J.; Fung, E.; Schlecht, U.; Davis, R. W.; Giaever, G.; St. Onge, R. P.; Deutschbauer, A.; Nislow, C. Gene Annotation and Drug Target Discovery in *Candida Albicans* with a Tagged Transposon Mutant Collection. *PLoS Pathogens* **2010**, *6* (10), e1001140.
- (41) Fu, C.; Zhang, X.; Veri, A. O.; Iyer, K. R.; Lash, E.; Xue, A.; Yan, H.; Revie, N. M.; Wong, C.; Lin, Z.-Y.; Polvi, E. J.; Liston, S. D.; VanderSluis, B.; Hou, J.; Yashiroda, Y.; Gingras, A.-C.; Boone, C.; O’Meara, T. R.; O’Meara, M. J.; Noble, S. Leveraging Machine Learning Essentiality Predictions and Chemogenomic Interactions to Identify Antifungal Targets. *Nature Communications* **2021**, *12* (1).
- (42) Brito Querido, J.; Sokabe, M.; Kraatz, S.; Gordiyenko, Y.; Skehel, J. M.; Fraser, C. S.; Ramakrishnan, V. Structure of a Human 48S Translational Initiation Complex. *Science* **2020**, *369* (6508), 1220–1227.
- (43) Browning, K. S.; Gallie, D. R.; Hershey, J. W. B.; Hinnebusch, A. G.; Maitra, U.; Merrick, W. C.; Norbury, C. Unified Nomenclature for the Subunits of Eukaryotic Initiation Factor 3 | This Letter Arises from the Cold Spring Harbor Translational Control Meeting Held on September 6–10 2000 in Cold Spring Harbor, NY, USA. *Trends in Biochemical Sciences* **2001**, *26* (5), 284.
- (44) Gerami-Nejad, M.; Forche, A.; McClellan, M.; Berman, J. Analysis of Protein Function in Clinical *C. Albicans* Isolates. *Yeast* **2012**, *29* (8), 303–309.
- (45) Roche Life Science Products. High Pure Plasmid Isolation Kit, 11th ed.; *Sigma-Aldrich*. **2017**, 3-15.
- (46) England Biolabs, N. PCR with Q5® High-Fidelity 2X Master Mix (M0492) V2. **2020**.
- (47) Roche Life Science Products. High Pure PCR Product Purification Kit, 19th ed.; *Sigma-Aldrich*. **2018**, 3-14.

- (48) Zhao, X.; Li, G.; Liang, S. Several Affinity Tags Commonly Used in Chromatographic Purification. *Journal of Analytical Methods in Chemistry* **2013**, *2013*, 1–8.
- (49) Shen, J.; Guo, W.; Kohler, J. R. CaNAT1, a Heterologous Dominant Selectable Marker for Transformation of *Candida Albicans* and Other Pathogenic *Candida* Species. *Infection and Immunity* **2005**, *73* (2), 1239–1242.
- (50) Khoshnevis, S.; Hauer, F.; Milón, P.; Stark, H.; Ficner, R. Novel Insights into the Architecture and Protein Interaction Network of Yeast EIF3. *RNA* **2012**, *18* (12), 2306–2319.
- (51) Acker, M. G.; Kolitz, S. E.; Mitchell, S. F.; Nanda, J. S.; Lorsch, J. R. Reconstitution of Yeast Translation Initiation. *Methods in Enzymology* **2007**, *430*, 111–145.
- (52) Young, D. J.; Guydosh, N. R. Hcr1/EIF3j Is a 60S Ribosomal Subunit Recycling Accessory Factor in Vivo. *Cell Reports* **2019**, *28* (1), 39–50.
- (53) Fraser, C. S.; Lee, J. Y.; Mayeur, G. L.; Bushell, M.; Doudna, J. A.; Hershey, J. W. B. The J-Subunit of Human Translation Initiation Factor EIF3 Is Required for the Stable Binding of EIF3 and Its Subcomplexes to 40 S Ribosomal Subunits in Vitro. *Journal of Biological Chemistry* **2004**, *279* (10), 8946–8956.
- (54) Takizawa, P. A.; Vale, R. D. The Myosin Motor, Myo4p, Binds Ash1 mRNA via the Adapter Protein, She3p. *Proceedings of the National Academy of Sciences* **2000**, *97* (10), 5273–5278.
- (55) Landers, S. M.; Gallas, M. R.; Little, J.; Long, R. M. She3p Possesses a Novel Activity Required for ASH1 mRNA Localization in *Saccharomyces Cerevisiae*. *Eukaryotic Cell* **2009**, *8* (7), 1072–1083.
- (56) Homma, M. K.; Wada, I.; Suzuki, T.; Yamaki, J.; Krebs, E. G.; Homma, Y. CK2 Phosphorylation of Eukaryotic Translation Initiation Factor 5 Potentiates Cell Cycle Progression. *Proceedings of the National Academy of Sciences* **2005**, *102* (43), 15688–15693.
- (57) Gandin, V.; Masvidal, L.; Cargnello, M.; Gyenis, L.; McLaughlan, S.; Cai, Y.; Tenkerian, C.; Morita, M.; Balanathan, P.; Jean-Jean, O.; Stambolic, V.; Trost, M.; Furic, L.; Larose, L.; Koromilas, A. E.; Asano, K.; Litchfield, D.; Larsson, O.; Topisirovic, I. MTORC1 and CK2 Coordinate Ternary and EIF4F Complex Assembly. *Nature Communications* **2016**, *7* (1).
- (58) Borgo, C.; Franchin, C.; Salizzato, V.; Cesaro, L.; Arrigoni, G.; Matricardi, L.; Pinna, L. A.; Donella-Deana, A. Protein Kinase CK2 Potentiates Translation Efficiency by Phosphorylating EIF3j at Ser127. *Biochimica et Biophysica Acta (BBA) - Molecular Cell Research* **2015**, *1853* (7), 1693–1701.
- (59) Dennis, M. D.; Person, M. D.; Browning, K. S. Phosphorylation of Plant Translation Initiation Factors by CK2 Enhances the in Vitro Interaction of Multifactor Complex Components. *Journal of Biological Chemistry* **2009**, *284* (31), 20615–20628.
- (60) Das, S.; Maitra, U. Functional Significance and Mechanism of EIF5-Promoted GTP Hydrolysis in Eukaryotic Translation Initiation. *Progress in Nucleic Acid Research and Molecular Biology* **2001**, *70*, 207–231.
- (61) Wang, J.; Johnson, A. G.; Lapointe, C. P.; Choi, J.; Prabhakar, A.; Chen, D.-H.; Petrov, A. N.; Puglisi, J. D. EIF5B Gates the Transition from Translation Initiation to Elongation. *Nature* **2019**, *573* (7775), 605–608.
- (62) Valášek, L. S.; Zeman, J.; Wagner, S.; Beznosková, P.; Pavlíková, Z.; Mohammad, M. P.; Hronová, V.; Herrmannová, A.; Hashem, Y.; Gunišová, S. Embraced by EIF3: Structural

- and Functional Insights into the Roles of EIF3 across the Translation Cycle. *Nucleic Acids Research* **2017**, *45* (19), 10948–10968.
- (63) Danan, C.; Manickavel, S.; Hafner, M. PAR-CLIP: A Method for Transcriptome-Wide Identification of RNA Binding Protein Interaction Sites. *Methods in Molecular Biology* **2021**, 167–188.
- (64) Yip, K. M.; Fischer, N.; Paknia, E.; Chari, A.; Stark, H. Atomic-Resolution Protein Structure Determination by Cryo-EM. *Nature* **2020**, 1–5.
- (65) Yin, Y.; Long, J.; Sun, Y.; Li, H.; Jiang, E.; Zeng, C.; Zhu, W. The Function and Clinical Significance of EIF3 in Cancer. *Gene* **2018**, *673*, 130–133.
- (66) Li, J.; Yu, W.; Ge, J.; Zhang, J.; Wang, Y.; Wang, P.; Shi, G. Targeting EIF3f Suppresses the Growth of Prostate Cancer Cells by Inhibiting Akt Signaling. *Oncotargets and Therapy* **2020**, *Volume 13*, 3739–3750.